ACS APPLIED MATERIALS & INTERFACES

Research Article

www.acsami.org

Factors that Affect Pickering Emulsions Stabilized by Graphene Oxide

Yongqiang He,[†,‡] Fei Wu,*[,‡] Xiying Sun,[‡] Ruqiang Li,[‡] Yongqin Guo,[‡] Chuanbao Li,[‡] Lu Zhang,[‡] Fubao Xing,[‡] Wei Wang,[§] and Jianping Gao*[,‡]

[†]Department of Applied Chemistry, Yuncheng University, Yuncheng 044000, People's Republic of China

[‡]School of Science, [§]School of Chemical Engineering, Tianjin University, Tianjin 300072, People's Republic of China

Supporting Information

ABSTRACT: Stable Pickering emulsions were prepared using only graphene oxide (GO) as a stabilizer, and the effects of the type of oil, the sonication time, the GO concentration, the oil/water ratio, and the pH value on the stability, type, and morphology of these emulsions were investigated. In addition, the effects of salt and the extent of GO reduction on emulsion formation and stability were studied and discussed. The average droplet size decreased with sonication time and with GO concentration, and the emulsions tended to achieve good stability at intermediate oil/water ratios and at low pH values. In all solvents, the emulsions were of the oil-in-water type, but interestingly, some water-in-oil-in-water (w/o/w) multiple emulsion droplets were also observed with low GO concentrations, low pH values, high oil/water ratios, high salt concentrations, or moderately reduced GO in the benzyl chloride−water system. A Pickering emulsion stabilized by Ag/GO was also prepared, and its catalytic performance for the reduction of 4-nitrophenol was investigated. This research paves the way for the fabrication of graphene-based functional materials with novel nanostructures and microstructures.

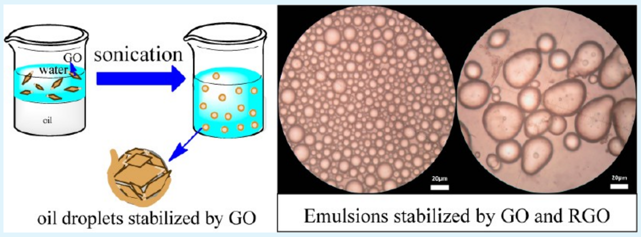

oil droplets stabilized by GO

Emulsions stabilized by GO and RGO

KEYWORDS: *Pickering emulsion, graphene oxide, sonication method, hydrophilic properties, multiple emulsion*

1. INTRODUCTION

Since the pioneering work of Ramsden[1] and Pickering,[2] Pickering emulsions or solid-stabilized emulsions, which refer to solid colloidal emulsions stabilized by solid particles instead of organic surfactants, have attracted interest because of their potential applications in the food,[3,4] cosmetics,[5] and pharmaceutical fields,[6,7] especially where the presence of surfactants is unwelcome. Compared to classical surfactants, smaller amounts of colloidal particles are required to create droplets with narrow size distributions, which can then produce emulsions with excellent stability.[8] Therefore, colloidal particles are considered environmentally friendly and cost-saving emulsifiers.

In Pickering emulsions, solid particles have been shown to assemble at the fluid interface because of the reduced total interfacial energy that occurs when part of the liquid−liquid or liquid−vapor interface is replaced with a liquid−particle interface.[9−11] This results in the dispersed droplets of one immiscible liquid steadily forming in another liquid. The properties of the solid particles, such as their concentration, wettability, shape, and size, and the interactions between the particles play a major role in Pickering behavior.[12,13] Among these factors, the wettability of the particle has been proven to be a key factor in the type of Pickering emulsion and its properties. Whether the particles are more hydrophilic or more hydrophobic determines whether they tend to stabilize oil-in-water (o/w) or water-in-oil (w/o) emulsions, respectively. If the particles are completely wetted by water or oil, they may remain in a single phase and a stable emulsion will fail to form.[14−17] An oil-in-water-in-oil (o/w/o) or a water-in-oil-in-water (w/o/w) multiple emulsion can be obtained with a mixture of hydrophilic and hydrophobic surfactants or with a combination of small solid particles and surfactants. Similarly, multiple emulsions can be formed by adding two types of particles with different hydrophobicities to oil and water mixtures. Binks prepared both types of extremely stable multiple emulsions using a mixture of silica particles that differed in SiOH content by only 25%.[12] In some cases, multiple emulsions can form around phase inversion of emulsions in a system containing only one particle type.[18] Factors that induce phase inversion cause differences in the wetting behavior of the particles, which helps to stabilize multiple emulsions.[19] The formation of multiple emulsions is also associated with particle shape. Nonomura et al. found that microbowls exhibited anomalous emulsification behavior and formed multiple/nonspherical emulsions due to the holes on the particle surfaces.[20]

Received: February 14, 2013
Accepted: May 6, 2013
Published: May 6, 2013

In addition, particles with smaller sizes and with weak flocculation affect the stability of the emulsions.[21] Binks and Lumsdon proved that the stability of emulsions containing silica particles could be improved by controlling the extent of particle flocculation with simple electrolytes.[22] This was attributed to the reduction of the electrostatic repulsions between the particles, which allowed a denser film to form around the oil drops, thus increasing their stability to coalescence. To date, a remarkable variety of solid particles, such as polymer micelles,[23,24] latex particles,[25] inorganic particles,[26−28] proteins,[29,30] and even bacterial cellulose nanocrystals,[31] have been used for the stabilization of Pickering emulsions.

Graphene oxide (GO) is a derivative of graphene. GO is obtained by the oxidation of graphite powder and has been the subject of a great deal of research due to its unique structure and its potential to be used in the cost-effective large-scale production of graphene-based materials.[32,33] Each GO sheet is composed of a 2D lattice of partially broken sp^2-bonded carbon networks with phenol, hydroxyl, and epoxide groups on the basal planes and carboxylic acid groups at the edges. This makes GO an amphoteric (hydrophilic−hydrophobic) molecule. Kim et al. reported the assembly behavior of GO at air−water, liquid−liquid, and liquid−solid interfaces and proved that GO could behave like a colloidal surfactant.[34] Gudarzi and Sharif have reported the preparation of polymer/GO microspheres by in situ polymerization using GO as a colloidal surfactant.[35] The resulting nanocomposites with 0.3 wt % graphene showed improved thermal stability and stiffness compared to the neat resin.

In this paper, the behavior of Pickering emulsions stabilized by GO was analyzed in detail. The effects of different conditions on the properties of the Pickering emulsions stabilized by GO were investigated extensively. The optimum experimental conditions for Pickering emulsions stabled by only GO (no added electrolytes or surfactants) is proposed, which provides guidance for the fabrication of functional materials in future works. Furthermore, the effect of adding different electrolytes to improve the emulsion stability by controlling the extent of particle flocculation was investigated. A Pickering emulsion stabilized by Ag/GO was also prepared, and its catalytic performance for the reduction of 4-nitrophenol was investigated. Because Pickering emulsions can be used as templates to design new functional hybrid materials,[36,37] this research paves the way for wide-scale applications of graphene-based functional materials with novel nanostructures and microstructures.

2. EXPERIMENTAL SECTION

2.1. Materials. Graphite was obtained from the Huadong Graphite Processing Factory. Potassium permanganate, sodium nitrate, concentrated sulfuric acid, 30% hydrogen peroxide, hydrochloric acid, sodium chloride, magnesium chloride hexahydrate, glucosamine, silver nitrate, sodium borohydride, and the organic solvents were all purchased from Tianjin Chemical Technology Co. All chemicals were analytical grade and used as received.

2.2. Preparation of the GO Aqueous Suspension. GO was prepared from purified natural graphite by a modified Hummers method.[38] Briefly, concentrated H_2SO_4 (23 mL) was added to a 250 mL flask filled with graphite (1 g) at 0 °C (ice bath), followed by the addition of $NaNO_3$ (0.5 g) and solid $KMnO_4$ (3 g) with stirring. After increasing the temperature to 35 °C, excess deionized water was added to the mixture, and the temperature was then increased to 90 °C. Finally, 30% H_2O_2 was added until the color of the mixture turned to brilliant yellow. The mixture was filtered and washed three times with 5% HCl aqueous solution to remove metal ions and then washed with distilled water to remove the acid. The resulting filter cake was dried in air and dispersed into water. A yellow-brown aqueous suspension of GO sheets was obtained after ultrasonic treatment.

2.3. Preparation of Pickering Emulsions Stabilized by GO at Different Conditions. The type of organic solvent, sonication time, GO concentration, oil/water ratio, and pH value all determine the properties of the resulting emulsion. Therefore, these experimental conditions were varied in order to investigate their effects on the emulsion stability. To investigate the effect of the electrolyte on the emulsion stability, salts of different valences were added to the initial aqueous dispersions. GO was reduced by glucosamine at 80 °C for different lengths of times to obtain suspensions of slightly reduced GO, and these were then used to prepare Pickering emulsions. An aqueous dispersion of GO was mixed with an organic solvent and sonicated with an ultrasonic device with a dipping probe close to the surface to form Pickering emulsions. For example, for the benzyl chloride−water emulsion with an oil/water ratio of 1/1, 10 mL of benzyl chloride was added to 10 mL of 1 mg mL^{-1} aqueous GO suspension in a 30 mL vial. The mixture was sonicated at 160 W for 3 min and allowed to stand for a period of time before characterization.

2.4. Preparation of Pickering Emulsions Stabilized by Ag/GO and the Catalytic Reduction of 4-Nitrophenol. First, 15 mL of $AgNO_3$ aqueous solution (0.4 mg/mL) was mixed with 2 mL of GO suspension (8 mg/mL). The mixture was stirred for 15 min at 84 °C, during which time the Ag nanoparticles were deposited on the surface of the GO sheets to form Ag/GO. A 4 mL portion of benzyl chloride was then added to 8 mL of the Ag/GO suspension, and the mixture was sonicated at 160 W for 3 min to prepare a Pickering emulsion.

The emulsion was then used to catalyze the reduction of 4-nitrophenol (4-NP). First, 5 mL of aqueous 4-NP solution (1.54×10^{-3} M) was mixed with 1 mL of freshly prepared aqueous $NaBH_4$ solution (0.88 M), and a deep yellow solution was formed. A 75 μL portion of the prepared emulsion was then added to the solution, and when the solution became colorless, it indicated that the reaction was finished. The reaction progress was monitored by UV−vis spectroscopy at 400 nm (the characteristic peak of 4-nitrophenol). After the reaction was finished, the supernatant was removed. New reactants were added to the catalyst residue that had settled on the bottom of the vial, and another cycle of the reaction was performed.

2.5. Characterization. The zeta potentials of the GO dispersions at different pH values and salt concentrations were measured using a Malvern Zetasizer Nano ZS at 25 °C. The photos of the emulsions stabilized by GO were recorded with a digital camera (COOLPIX S620, Nikon, Tokyo, Japan). The optical micrographs of the prepared emulsions on transparent glass slides were taken using a BM2000 microscope (Nanjing Jiangnan Novel Optics Co., Ltd., Nanjing, China) immediately after each preparation. The average sizes and size distributions of the emulsion droplets were determined based on the images of the emulsion droplets using Nano Measurer 1.2 software. The volume fraction of the stable emulsion was calculated by dividing the height of the emulsion phase by the total height of the initial emulsion. The emulsion samples on the glass slides were first dried in air and were then coated by a thin layer of gold. The morphology of the dry residue on the glass slide was examined using scanning electron microscopy (SEM, FEI NanoSEM 430) with a 5 kV accelerating voltage. The morphology of Ag/GO was characterized using transmission electron microscopy (TEM, Philips Tecnai G2 F20) at 200 kV.

3. RESULTS AND DISCUSSION

3.1. Pickering Emulsion Stabilized by Graphene Oxide. A stable GO aqueous suspension was prepared from natural graphite by a modified Hummers method.[38] The aqueous suspension is stable for several months, and no precipitation occurs. Pristine graphite is extremely hydrophobic; however, hydroxyl, epoxy, and carboxylic acid groups are introduced onto the GO sheets during oxidation.[39] This was confirmed by transmission electron microscopy (TEM), atomic

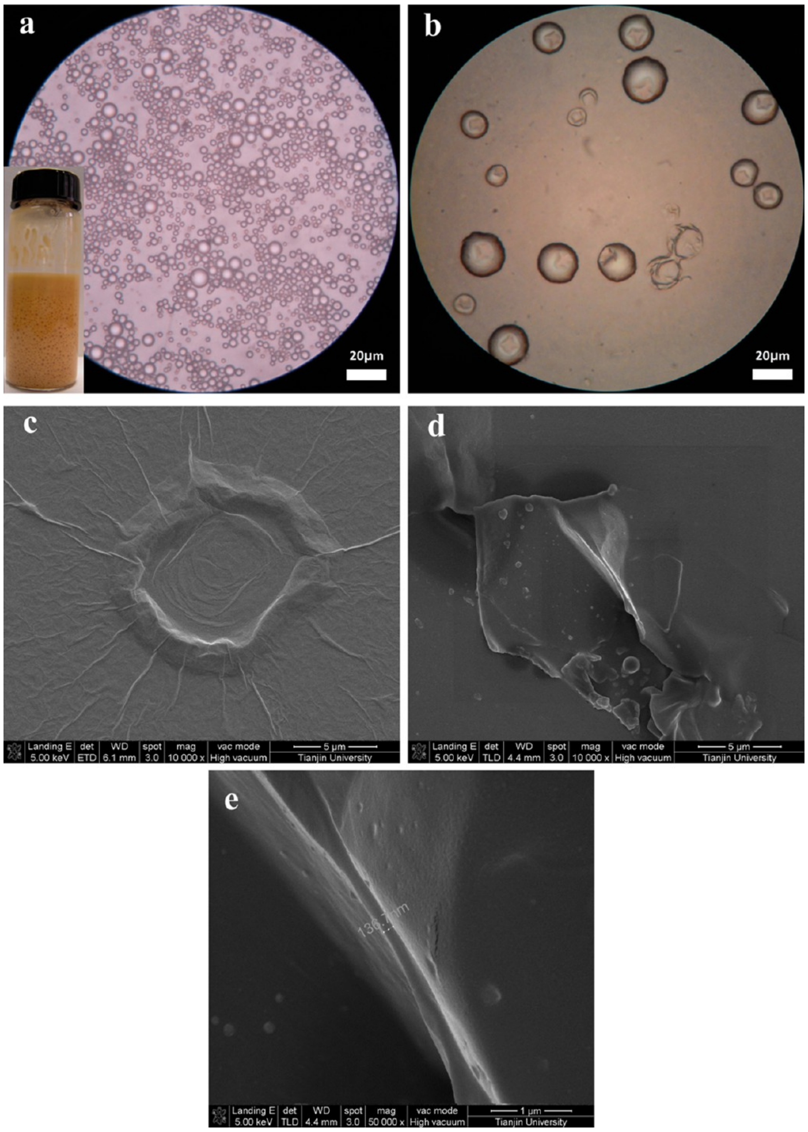

Figure 1. (a) Optical micrograph and photograph of benzyl chloride-in-water Pickering emulsion stabilized by graphene. (b) Optical micrograph of the residues of the emulsion droplets after drying. (c) SEM image of a dried droplet. (d) SEM image of the edge of a dried droplet cut by a sharp blade and (e) the magnification of the folded edge in (d). GO concentration: 3 mg mL^{-1}. Oil/water ratio: 1:1.

force microscopy (AFM), Fourier transform infrared spectroscopy (FT-IR spectra), X-ray diffraction spectroscopy (XRD), and X-ray photoelectron spectroscopy (XPS) (see the Supporting Information, Figures S1−S5).

The TEM images demonstrate that the GO sheets consist of one to several layers (Figure S1, Supporting Information). The thickness and lateral size of the GO sheets were determined by AFM (Figure S2, Supporting Information). The GO sheet is about 0.9 nm thick, which is consistent with the previously reported thickness for single-layered GO. In the AFM image, both small GO sheets of about 1 μm and large sheets of more than 2 μm are observed. The surface area of GO is 385 m^2/g according to the BET result.

The FT-IR spectrum of GO confirmed the oxidation of graphene (Figure S3, Supporting Information). The GO has peaks at 1725 cm^{-1} ($\nu_{C=O}$) from carbonyl and carboxylic groups and at 1042 cm^{-1} (ν_{C-O}) from carbonyl, carboxylic, and epoxy groups, which confirms the presence of oxygen-containing functional groups.

For the XRD patterns of graphite and GO (Figure S4, Supporting Information), the graphite has a strong diffraction peak at about 26.52°, which represents an interlayer distance of 0.34 nm. However, this peak disappears in GO, and a new weak diffraction peak for exfoliated GO at 11.4° with an interlay space (*d*-spacing) of 0.78 nm is observed. The large interlayer distance is attributed to the formation of hydroxyl, epoxy, and carboxyl groups, which causes the intercalation of water molecules and increases the distances between the layers.

The chemical composition of GO was characterized by XPS (Figure S5, Supporting Information). Binding energies of GO at 284.44 eV (C═C), 286.55 eV (C−O), and 288 0.47 eV (C═O) are observed. The percentage of O 1s in GO is about 25.9%, which indicates that there are many oxygen-containing functional groups on the GO sheets. These functional groups make GO partially hydrophilic, and the stable GO aqueous suspension can be used for the formation of Pickering emulsions.

Figure 1a shows the photographs and optical micrographs of an emulsion stabilized by GO. Clearly, the GO is a very good emulsifier that forms stable emulsions with benzyl chloride/water mixtures. The sizes of the emulsion droplets had a relatively homogeneous distribution, and most droplet were around 2−5 μm in diameter. The emulsion is stable for at least several months. Emulsion type was also inferred to be o/w by observing what happened when a drop of each emulsion was added to a volume of either pure oil or pure water.[40]

The close proximity of the emulsion droplets did not cause them to coalesce, which indicates that the presence of GO hinders coalescence and phase separation and thus efficiently stabilizes the emulsion. The reason the GO sheets behave this way is that the basal planes of the carbon networks and the three kinds of oxygen-containing functional groups that are on those planes endow the GO sheets with both hydrophilic and hydrophobic properties, which makes them act like a functional surfactant.

Studies on the wettability of GO have shown that the water contact angle is in the range of 62−68°,[41,42] much less than 90°, which demonstrates that GO is partially hydrophilic and tends to stabilize o/w emulsions because the particle surface resides more in water than in oil. This is consistent with our experimental results. The process of emulsification along with the GO absorption process at the interface of the two immiscible liquids leads to a reduction in the free energy of the system. The high surface area of the GO sheets enables them to be trapped at the interface and to wrap around the oil droplets.

Figure 1b shows the optical micrograph of the remains of the emulsion droplets after drying. As the emulsion was heated, the liquid phases of the emulsion were quickly volatilized and some small droplets coalesced into larger ones with denser and more rigid films of GO around them. These GO sheets remained in the shape of spheres, and dents formed on the surface when the liquid was completely removed. The details of the wrinkles and collapse can be seen in the SEM image in Figure 1c. The center and edges further collapsed onto the substrate due to the vacuum conditions during SEM observation. A hollow dried droplet cut by a sharp blade is shown in Figure 1d. This also proves that the self-assembly of GO occurred at the interface of the oil and water. As shown in Figure 1e, the thickness of the folded edge is 136.7 nm. Thus, the thickness of the GO film around the emulsion droplets is about 68.4 nm. Since the thickness for single-layered GO is about 0.9 nm according to the AFM image, it can be calculated that there are about 76 layers of GO sheets at the oil−water interface. Therefore, the GO is present as stacked layers instead of a single layer at the oil−water interface in the emulsions.

3.2. Effect of the Type of Oil on the Emulsions Stabilized by GO.

Pickering emulsions are affected by several factors, including the properties of the oil phases, the particle concentration, the oil/water ratio, and the sonication time. Several aromatic organic solvents and nonaromatic solvents were used as the oil phase to prepare Pickering emulsions, and the results are shown in Figure 2. All the emulsions were of the o/w type, and the stabilizing ability of GO for aromatic solvents (Figure 2a−f) was much greater than that for nonaromatic solvents (Figure 2g−l). This is indicated by the fact that, in general, for the aromatic solvents, a higher volume fraction of the oil was incorporated into the residual emulsion. This could be attributed to π−π interactions between the residual conjugate domains in the GO and the aromatic molecules, as illustrated in Figure 3.

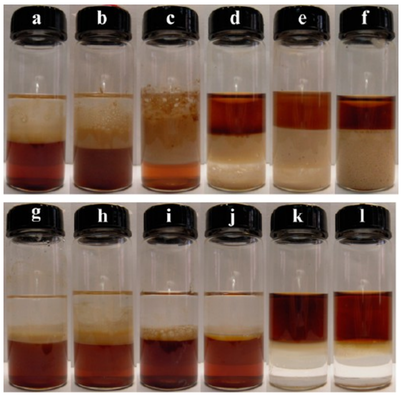

Figure 2. Photographs of Pickering o/w emulsions in different solvents stabilized by GO, taken 72 h after preparation: (a) benzene (0.879 g cm^{-3}), (b) benzene with dissolved naphthalene, (c) toluene (0.867 g cm^{-3}), (d) chlorobenzene (1.108 g cm^{-3}), (e) ethyl benzoate (1.045 g cm^{-3}), (f) benzyl chloride (1.100 g cm^{-3}), (g) 1-decanol (0.829 g cm^{-3}), (h) ethyl heptanoate (0.868 g cm^{-3}), (i) *n*-hexane (0.659 g cm^{-3}), (j) cyclohexane (0.779 g cm^{-3}), (k) tetrachloromethane (1.595 g cm^{-3}), and (l) chloroform (1.484 g cm^{-3}). GO concentration: 1 mg mL^{-1}. Oil/water ratio: 1:1. The mass density (at 20 °C) of each solvent is included after the name of the solvent.

Benzene did not behave as well in the Pickering emulsion as the other aromatic solvents that all had substituent groups on the benzene ring. This may be because GO is composed of partially broken sp^2-carbon networks and the substituent groups on the benzene rings can interact with the various groups at the edges of the GO, which results in stronger interactions between the GO and the solvent. On the other hand, adding naphthalene to benzene improved the stability of the emulsion (Figure 2b), which indicates that reagents with more aromatic rings have stronger π−π interactions with GO and thus produce emulsions with a higher stable volume fraction and with much smaller emulsion droplets (Figure S6, Supporting Information). This further proves that π−π interactions have a significant influence on the Pickering emulsions stabilized by GO and explains why aromatic solvents are beneficial for the formation of stable Pickering emulsions.

GO had a very low emulsification efficiency for nonaromatic solvents, but the situation for strongly polar oils and weakly polar oils is slightly different. GO tended to behave better for strongly polar oils, such as decanol and ethyl heptanoate (Figure 2g,h), than for nonpolar and weakly polar oils, such as *n*-hexane and cyclohexane (Figure 2i,j), which could be identified from the stable emulsion volume. Aromatic benzyl chloride was chosen as the oil phase to investigate the effects of other factors on the properties of Pickering emulsions stabled by GO.

3.3. Effect of Varying Sonication Time on the Emulsions Stabilized by GO.

The effect of sonication time on the morphology of the o/w Pickering emulsions was studied, and the results are shown in Figure 4 (the sonication power was kept constant at 160 W). As the sonication time increased, the average size of the emulsion droplets became smaller with a more uniform size distribution, and the stable emulsion volume increased slightly. The size distribution of the droplets was very large when the mixture was sonicated for only 1 min. When the sonication time was longer than 3 min, nearly all the emulsion droplets maintained their morphology very well. The average diameter of the emulsion droplets decreased to around 5 μm when the sonication time was 7 min (The

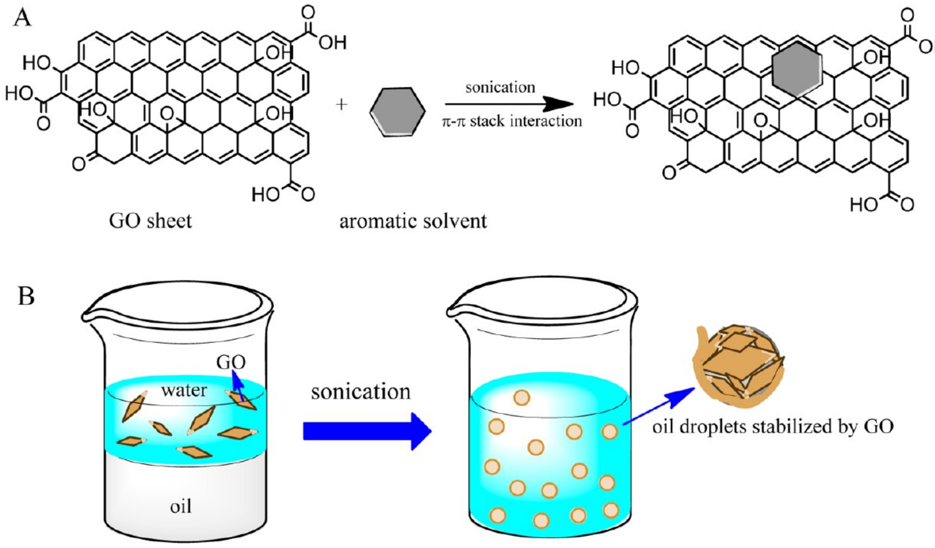

Figure 3. (A) Schematic illustration (not to scale) of $\pi-\pi$ interactions between the residual conjugate domains in the GO and the aromatic molecules. (B) Schematic illustration of the formation of Pickering emulsion droplets.

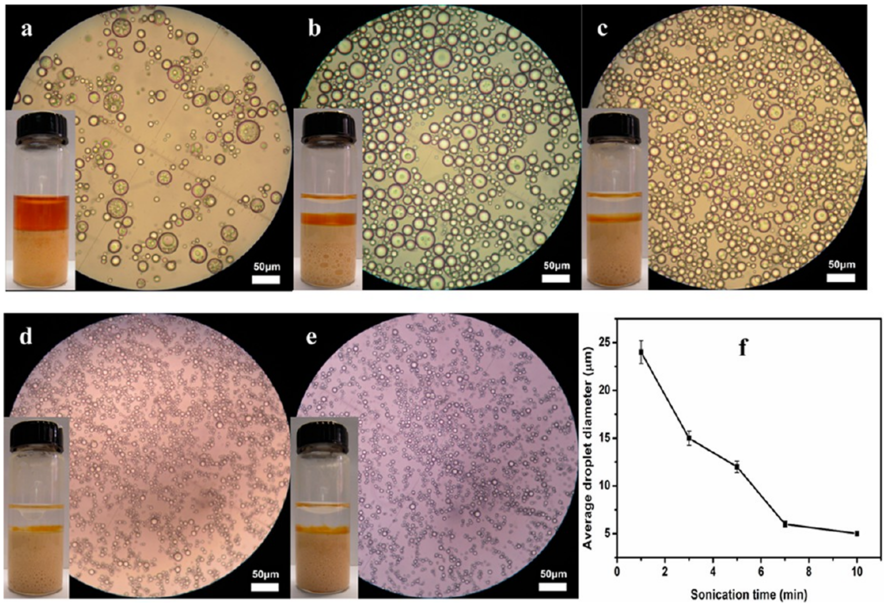

Figure 4. Optical micrographs and photographs 72 h after preparation of benzyl chloride-in-water Pickering emulsions stabilized by GO and treated with different sonication times: (a) 1, (b) 3, (c) 5, (d) 7, and (e) 10 min. (f) The average droplet diameter as a function of sonication time. GO concentration: 1 mg mL^{-1}. Oil/water ratio: 1:1.

optical micrographs of 7 and 10 min with a smaller scale bar are provided in Figure S7, Supporting Information). When the sonication time was further increased, the size of the emulsion droplets did not change much.

Increasing the sonication time caused more GO to associate with the stable emulsion, which can be seen from the color of the water phase. The brown color of the upper water phase shown in Figure 4a indicates that the GO only partially participated in the emulsion and much was left in the water. In Figure 4b–e, the color of the water phase is clearer and there is a GO layer deposited at the interface of the water/emulsion phase. The GO layer became thinner as the sonication time increased, which implies that more GO was involved in the formation of Pickering emulsions as the sonication time increased. Sonication can crush the GO sheets, making them smaller, so the effective GO size should decrease as the sonication time increases. This may be one of the reasons for the decrease in the size of the emulsion droplets with the sonication time. In addition, the efficiency of the emulsification was improved with the introduction of more energy to the emulsification process.

3.4. Effect of GO Concentration on the Emulsions Stabilized by GO.

Particle concentration is another important factor in the formation of Pickering emulsions, and it has a remarkable influence on the emulsion stability and on the average droplet size.[11] The surface energy of the system reduced with migration of GO from the aqueous dispersion onto the oil–water interface, and an increase in the surface area of GO causes a reduction in the free energy and makes the system more stable.[35] An increase of GO concentration within a certain range results in an increase of the total surface area of

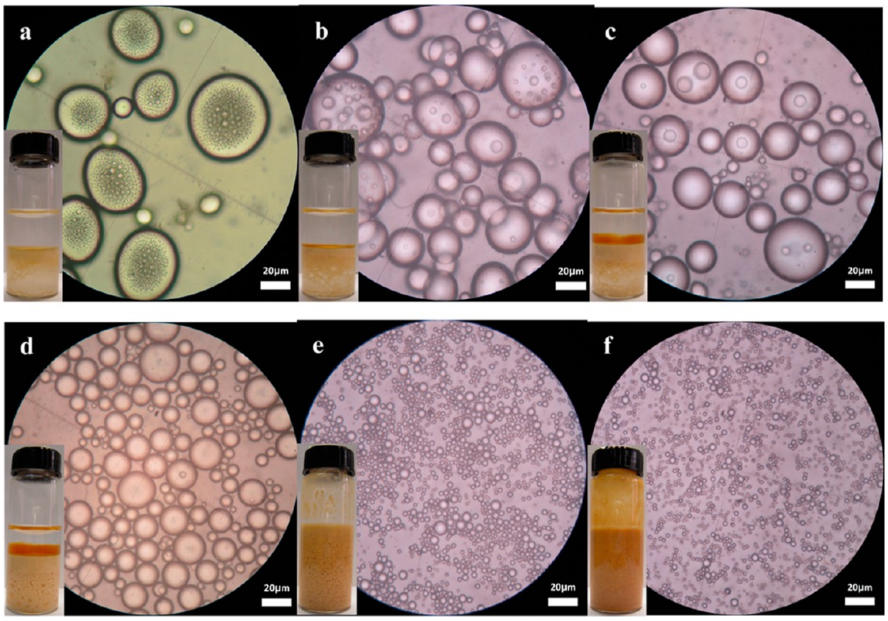

Figure 5. Optical micrographs and photographs 72 h after preparation of Pickering emulsions stabilized by GO at different concentrations: (a) 0.1, (b) 0.2, (c) 0.5, (d) 1, (e) 3, and (f) 6 mg/mL. Oil/water ratio: 1:1.

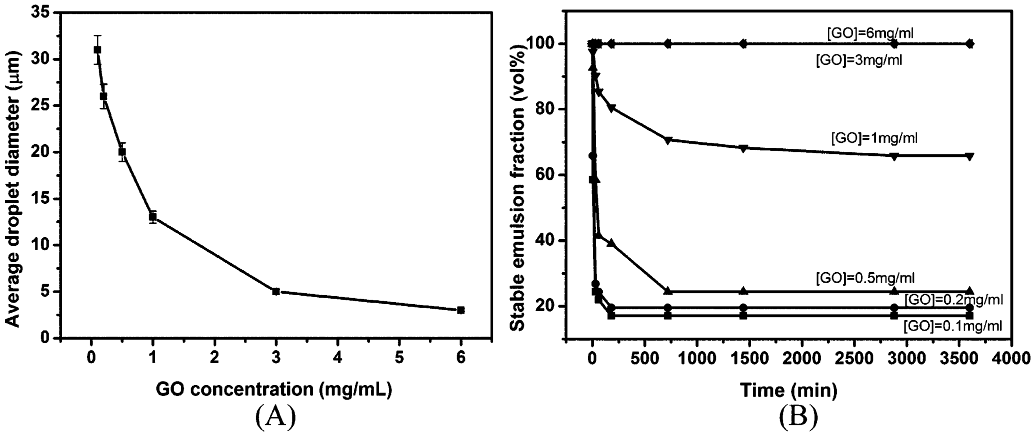

(A) (B)

Figure 6. (A) Average droplet diameter as a function of GO concentration. (B) Change in the volume fraction of the residual emulsion as a function of time for emulsions stabilized by different concentrations of GO.

GO assembling at the liquid–liquid interface, which facilitates the formation of Pickering emulsions with greater stabilities.

Figure 5 shows microscopy images and photographs taken for emulsions prepared with different GO particle concentrations, with the benzyl chloride/water volume ratio constant at 0.5. The quantification of these results is shown in Figure 6. As expected, the average droplet size decreased and the volume fraction of the residual emulsion increased as the particle concentration increased. Decreasing the solid particle concentration led not only to larger emulsion droplets but also to a greater heterogeneity in the droplet sizes and shapes, which signifies a less efficient emulsification under these conditions. For GO concentrations below 1 mg mL^{-1}, there was an almost linear increase in the average droplet diameter as a function of particle concentration (Figure 6A).When the concentration of GO was 0.1 or 0.2 mg mL^{-1}, the emulsions reached a stable state very quickly and the volume fraction of the residual emulsion was less than 20% (Figure 6B).

For concentrations greater than 3 mg mL^{-1}, there was no separated water phase and the average droplet diameter was less than 5 μm. Further increasing the concentration did not lead to an obvious change in the emulsification effect. At high GO concentrations, the increased viscosity of the continuous phase may also play a role in stabilizing very small droplets and the color of the emulsions became darker. The effect of GO concentration on the emulsion stability is greater than that of sonication time. The maximum stable emulsion volume was obtained with a high GO concentration after only 3 min of sonication, whereas the same effect cannot be achieved with a low GO concentration even when the sonication time is very long.

At GO concentrations lower than 1 mg mL^{-1}, multiple emulsion droplets (w/o/w) were observed, and for the lowest particle concentration (0.1 mg mL^{-1}), most of the emulsion droplets possessed this structure. Decreasing the GO concentration from 1 to 0.1 mg mL^{-1} led to an increase in the number of multi-emulsion droplets and also increased the number of inner w/o emulsion droplets per o/w emulsion droplet. The formation of multi-emulsions is likely related to the different hydrophilic properties of the GO sheets. Because

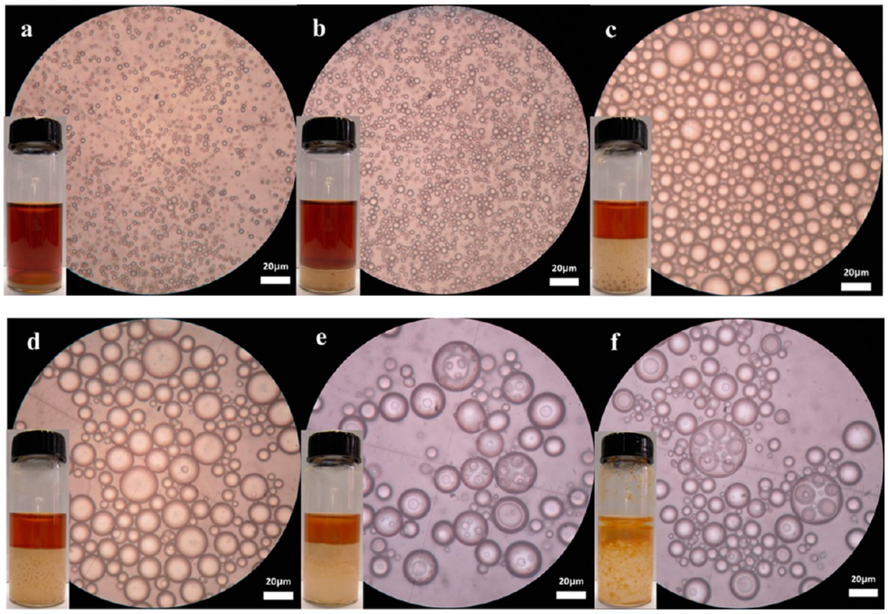

Figure 7. Optical micrographs and photographs 72 h after preparation of Pickering emulsions stabilized by GO at different oil/water ratios: (a) volume fractions of oil φ_o = 0.1, (b) φ_o = 0.2, (c) φ_o = 0.4, (d) φ_o = 0.5, (e) φ_o= 0.6, (f) φ_o = 0.8. GO concentration: 1 mg/mL.

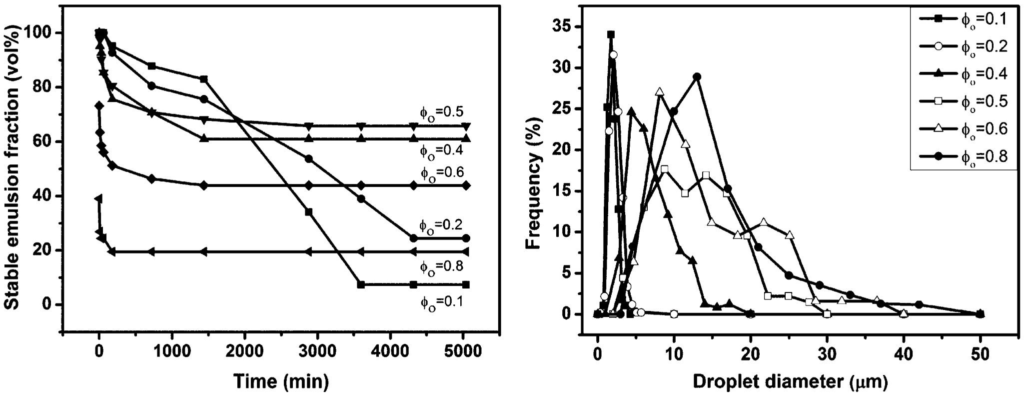

(A) (B)

Figure 8. (A) Change in the volume fraction of the residual emulsion as a function of time for the emulsions stabilized by GO at different oil fractions. (B) Distribution of droplet diameters after the preparation of benzyl chloride-in-water emulsions at different oil fractions.

the degree of oxidation and functionalization can be highly heterogeneous with the GO sheets, the amphiphilic properties of each GO sheet also can be different. A recent study on the composition of GO found that GO actually consisted of two distinct components noncovalently complexed together: the majority by mass being large functionalized graphene-like sheets together with small, more highly oxidized, fragments or debris.[43] Moreover, sonication can crush the GO particles, which would increase the amount of "debris" in the GO dispersion. The highly oxidized debris was much more hydrophilic than functionalized graphene-like sheets and acted as a surfactant to stabilize aqueous GO suspensions. At high GO concentrations, abundant oxidative debris was bound to functionalized graphene-like sheets and made the GO sheets very hydrophilic, whereas at low GO concentrations, few oxidative fragments were adhered to the functionalized graphene-like sheets and some GO sheets might show hydrophobic property. Such mixtures of hydrophobic and hydrophilic sheets might explain the appearance of both simple (o/w) and multiple (w/o/w) drops in the emulsion.

Interestingly, this multi-emulsion structure was only observed when benzyl chloride, chlorobenzene, or ethyl benzoate was used as the oil phase, and not when benzene, toluene, or nonaromatic solvents were used. The reason for this disparity is not quite clear yet, but it might be related to the significantly higher surface tension of chloride, chlorobenzene, and ethyl benzoate (~32−37 mN m^{-1}) compared with that of other solvents used (~18−29 mN m^{-1}).[17]

3.5. Effect of Varying the Oil/Water Ratio on the Emulsions Stabilized by GO.

The ratio of the dispersed phase and continuous phase is another important factor that affects the emulsion stability and sometimes even the emulsion type. The benzyl chloride-in-water emulsions prepared at different oil volume fractions are shown in Figure 7. There is a remarkable variation in the emulsion fraction as the oil/water ratio changes. As shown in Figure 8A, when $\varphi_o \leq 0.5$, the emulsion volume fraction increased as φ_o increased. However, when $\varphi_o > 0.5$, the opposite trend is observed. This is because fewer GO sheets were associated with the emulsions at higher φ_o and the emulsions became less stable to creaming and coalescence. In the cases of $\varphi_o < 0.4$, the time to reach a stable emulsion state was longer than when $\varphi_o \geq 0.4$. It was also found that an increase of GO concentration did not significantly affect the emulsion volume fraction when the oil phase was in excess of the water phase (Figure S8, Supporting Information). On the other hand, 100% of the volume fraction could not be stabilized in the emulsion when the GO concentration was 1 mg mL^{-1} with any value of φ_o. The maximum emulsion fraction is about 65% for $\varphi_o = 0.5$.

The emulsion droplet size increased and the size distribution became larger with increasing amounts of the oil phase, as shown in Figure 8B. The emulsion droplets possessed the smallest diameters, and particle distribution at $\varphi_o= 0.1$ and the largest were seen at $\varphi_o= 0.8$. Phase inversions of the emulsions from o/w to w/o did not occur at high values of φ_o (>0.5). However, interestingly, many w/o/w or even o/w/o/w multi-emulsion droplets began to appear when φ_o was higher than 0.5. Since fewer GO sheets were available to participate in the emulsions at higher oil volume fractions, this may also be attributed to the difference in the hydrophilicities of different GO sheets, similar to the situation at low GO concentration.

3.6. Effect of Varying the pH on the Emulsions Stabilized by GO. Varying the pH changes the hydrophobicity and hence the wettability of the particles that possess ionizable surface groups. Therefore, the adsorption behavior of the particles at the interface and sometimes the emulsion type can be controlled by varying the pH. A chargeable surface has the maximum hydrophobicity at conditions near its point of zero charge.[12] The zeta potentials of GO in water as a function of pH are shown in Figure 9. The GO is negatively charged, and the magnitude of the zeta potential increased with increasing pH. Therefore, the electrostatic repulsions between the charged GO sheets increased as the pH increased. As the pH increased, the GO sheets with abundant $-COOH$ groups on their edges became increasingly charged through dissociation ($-COO^-$), which increased their wettability by water and made them more hydrophilic. This is unfavorable for the formation of Pickering emulsions. This is verified in the benzyl chloride−water system.

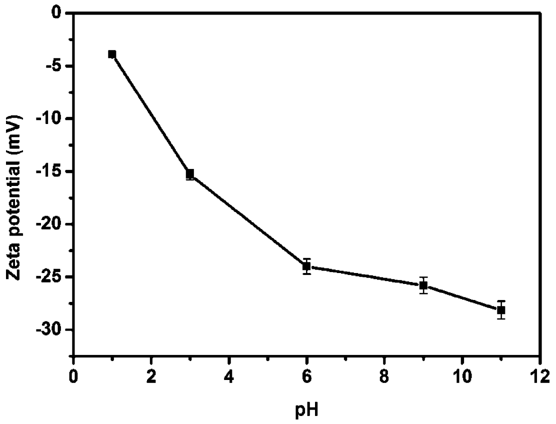

Figure 9. Zeta potentials of 1 mg/mL GO dispersed in water at different pH values.

As shown in Figure 10, the pH had a significant influence on the volume fraction of the residual emulsion. The stable emulsion volume decreased as the pH increased. At about pH 1, the emulsion fraction reached its maximum volume of about 75% and the color of the water phase was clear, indicating that nearly all the GO sheets in the dispersion were associated with the emulsification. As the pH increased, fewer GO sheets were transferred to the emulsion and the water phase became increasingly dark. When the pH was around 11, the emulsion fraction was reduced to less than 20%, showing poor emulsification.

The effect of pH on the droplet size was not distinct, but the interesting phenomenon of w/o/w multi-emulsion droplets was again observed for relatively low pH values. The number of multi-emulsion droplets decreased as the pH increased, and none were found at around pH 11. This is likely due to the effect of pH on the hydrophilic−lipophilic balance in the GO sheets. When the pH was as high as 11, the GO was rendered much more hydrophilic and all the emulsion droplets were o/w. In contrast, at low pH values, the initial hydrophilicity of the GO sheets was weakened to different extents and the differences in the hydrophilic properties led to the formation of w/o/w multiple emulsion droplets.

3.7. Effect of Salt on the Emulsions Stabilized by GO. The effects of salt on the emulsions stabilized by GO (1 mg mL^{-1}) were investigated. The appearance of the 1:1 benzyl chloride−water emulsions stabilized by GO with different NaCl concentrations and the optical micrographs of these emulsions are shown in Figure 11. The water phase gradually became paler and turned colorless as the NaCl concentration was increased from 0.1 to 50 mM (Figure 11a−e), which indicates that the efficiency of emulsification improved as the salt concentration increased. The emulsion droplet sizes passed through a minimum at 10−20 mM NaCl and then increased with NaCl concentration (Figure 12A). The maximum emulsion fraction was about 78% at a NaCl concentration of around 300 mM. In addition, more w/o/w multiple droplets began to appear at this concentration and almost all the emulsion droplets possessed multiple structures at 1000 mM NaCl (Figure 11g−i). These results show that adding salt to the systems improves the stability of emulsions and a high salt concentration contributes to the formation of the multi-emulsions.

Next, how the salt concentration affects the emulsion stability and the type of emulsion will be discussed. The salt influences the initial state of the GO dispersion. Both the carboxylic acid and hydroxyl groups in GO are candidates for charge screening when the salt is added. The effect of the salt concentration on the zeta potential of the GO dispersions was investigated. The variation of zeta potential with NaCl and $MgCl_2$ concentration is shown in Figure 12B. The zeta potentials gradually decreased in magnitude as the NaCl concentration increased, and when the NaCl concentration reached 1000 mM, the potential approached 0 mV (but still stayed negative).

For $MgCl_2$, the zeta potentials decreased in magnitude more rapidly as the concentration increased and the negative charges on GO surfaces were totally neutralized around a concentration of 300 mM (+0.171 mV). At even higher $MgCl_2$ concentrations, the zeta potential became positive. In summary, the electrostatic repulsions between the charged GO sheets were, in general, reduced by the addition of salt, which lead to aggregation or even flocculation of the GO sheets. Thus, the effective GO particle size increased with salt concentration and the hydrophobicity of the charged solid surfaces was changed.[40]

It has been shown that the droplet size of Pickering emulsions increases with particle size.[19] Therefore, the droplet sizes of the Pickering emulsions stabilized by the GO sheets should increase with salt concentration. However, this was not

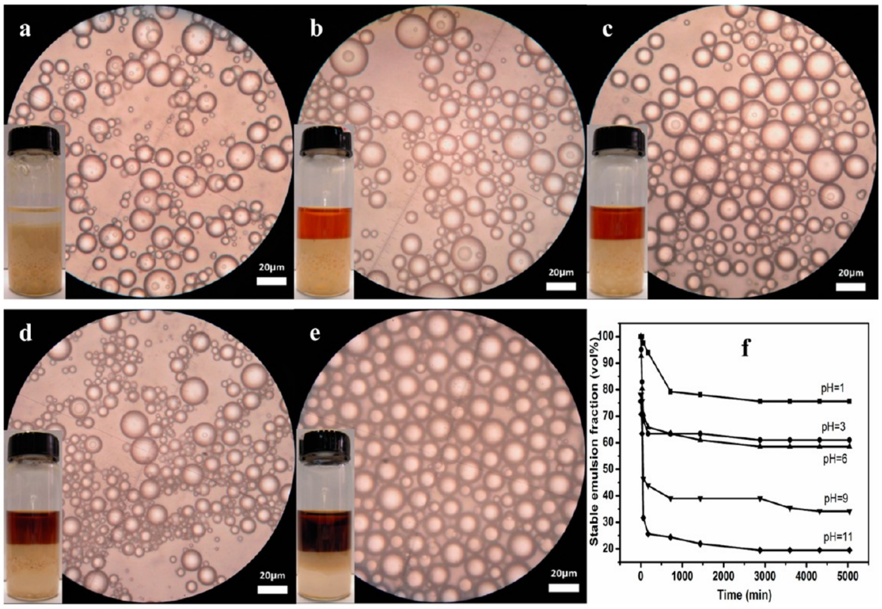

Figure 10. Optical micrographs and photographs 72 h after preparation of Pickering emulsions stabilized by GO at different pH values: (a) pH = 1, (b) pH = 3, (c) pH = 6, (d) pH = 9, (e) pH = 11. (f) Change in the volume fraction of the residual emulsion as a function of time at different pH values. GO concentration: 1 mg/mL. Oil/water ratio: 1:1.

the observed trend. The emulsion droplet sizes passed through a minimum at 10−20 mM NaCl and then increased at higher concentrations of NaCl. When the salt concentration is lower than 20 mM, the GO sheet folds and interacts with itself, which makes the sheet thicker and smaller.[44] This could be the origin of the minimum in the average drop size seen in Figure 12A. For salt concentrations above 20 mM, intersheet aggregation is prevalent, which makes the sheets even thicker and larger. This is responsible for the increase in the average drop size. In addition, there was a further increase in the hydrophobicity of the larger GO sheets because the edge-to-area ratio decreased as the size increased and the charge density resulting from the ionizable −COOH edge groups also decreased.[34] These are the reasons why the emulsion stability begins to increase drastically from 20 mM NaCl.

An increase in viscosity also helps to enhance emulsion stability, so moderate flocculation is favorable for the formation of stable emulsions. The emulsion volume reached a peak at 300 mM NaCl. However, the stability began to decrease when the salt concentration was further increased. The reason for the decreased stability may be the increase in floc size and in the extent of flocculation of the GO sheets as the salt concentration increased, which reduces the coverage of the droplets by GO.[45] In general, the hydrophobicity of the surface significantly increases at higher salt concentrations and the differences in the amphiphilic property of GO sheets help to stabilize multiple emulsions. When the salt concentration is higher, these changes become more significant, and therefore, more multiple emulsion droplets form. In the presence of the divalent electrolyte $MgCl_2$, similar behavior was observed (Figure S9, Supporting Information). The water phase became colorless at 10 mM, and multiple droplets began to appear in large quantities at 100 mM. Both of these concentrations are lower than the NaCl concentration required for the same effect, which shows that the divalent electrolyte had a more significant effect on the emulsion stabilized by GO.

3.8. Effect of the Extent of GO Reduction on the Property of the Emulsions. The amphiphilicity of GO can be tuned by the reduction of GO. As the oxygen-containing groups at the edges are reduced, GO becomes less hydrophilic. The extent of the reduction can be monitored by UV−vis absorption spectroscopy. The maximum absorption peak (λ_{max}) of a GO suspension is about 233.5 nm and red shifts to about 278.5 nm when GO is highly reduced;[46] therefore, the extent of the reduction is reflected by the amount of the red shift. The effect of the extent of GO reduction on the stability of the emulsion was investigated and is shown in Figure 13. When GO is transformed to highly reduced graphene oxide, it becomes extremely hydrophobic and precipitates from the water phase. Therefore, highly reduced GO cannot stabilize Pickering emulsions. However, a suspension of slightly reduced GO, which has fewer hydrophilic groups, can be used to prepare Pickering emulsions. The reduced GO is rendered more hydrophobic, which is favorable for the stability of the emulsions. The maximum stable emulsion volume reached 82.9% using slightly reduced GO as the emulsifier, which is higher than that using GO. However, the morphology of the emulsion droplets began to become irregular when the λ_{max} of the reduced GO was 252.6 nm, and at the same time, w/o/w multiple droplets appeared. The size of the reduced GO sheets may differ greatly from each other due to aggregation, and this leads to the diversity of droplets' shapes. The increase in the number of multiple droplets further verifies that the differences in the hydrophobicity of the sheets are the reason for the formation of multiple droplets.

3.9. The Reduction of 4-NP Catalyzed by the Emulsion Stabilized by Ag/GO. The TEM image of Ag/GO is shown in Figure 14a, and the image indicates that there are many Ag nanoparticles on the GO sheets. Pickering emulsion can be prepared using GO sheets loaded with Ag nanoparticles (Figure 14b). To evaluate the catalytic performance, the emulsion stabilized by Ag/GO was used in the catalytic reduction of 4-nitrophenol (4-NP) to 4-aminophenol (4-AP) with an excess

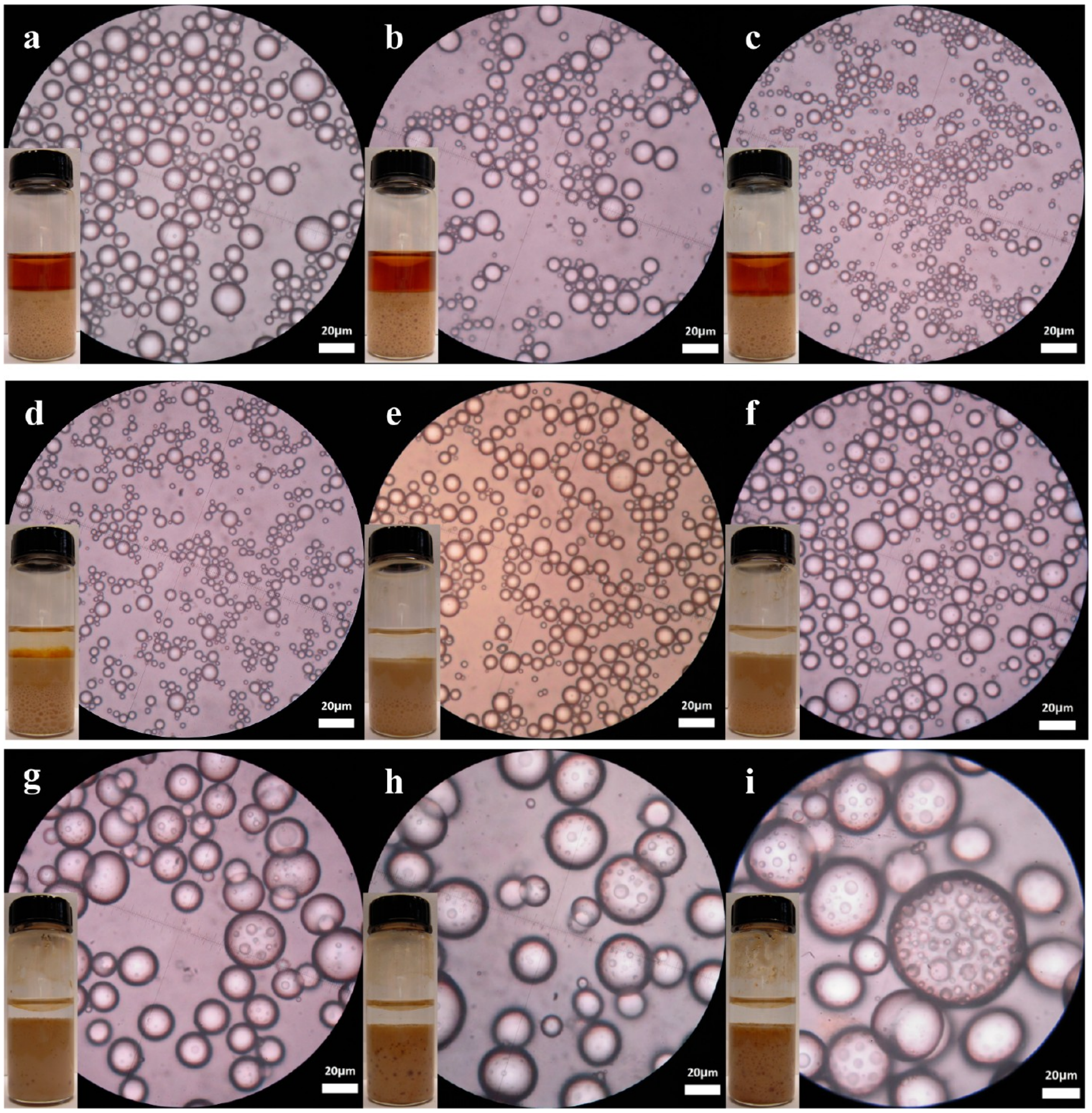

Figure 11. Optical micrographs and photographs 72 h after preparation of Pickering emulsions stabilized by GO with different NaCl concentrations. The concentrations of NaCl (mM) are (a) 0.1, (b) 1, (c) 10, (d) 20, (e) 50, (f) 100, (g) 300, (h) 500, and (i) 1000. GO concentration: 1 mg/mL. Oil/water ratio: 1:1.

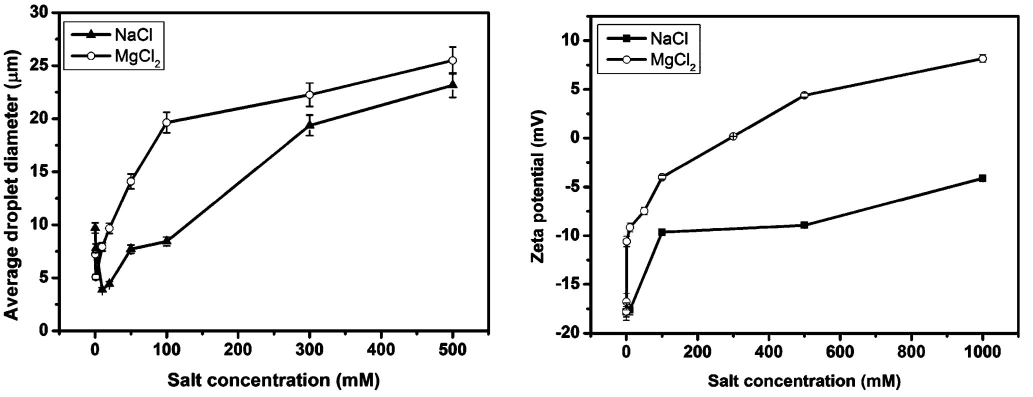

(A) (B)

Figure 12. (A) Average droplet diameter as a function of NaCl and $MgCl_2$ concentration. (B) Zeta potentials of 1 mg/mL GO dispersed in water with different concentrations of NaCl and $MgCl_2$.

amount of $NaBH_4$. The reduction process was monitored with UV−vis spectroscopy (Figure 15A). The absorbance of 4-NP at 400 nm decreased rapidly with a concomitant increase in the absorption peak at 300 nm, which is attributed to the reduction

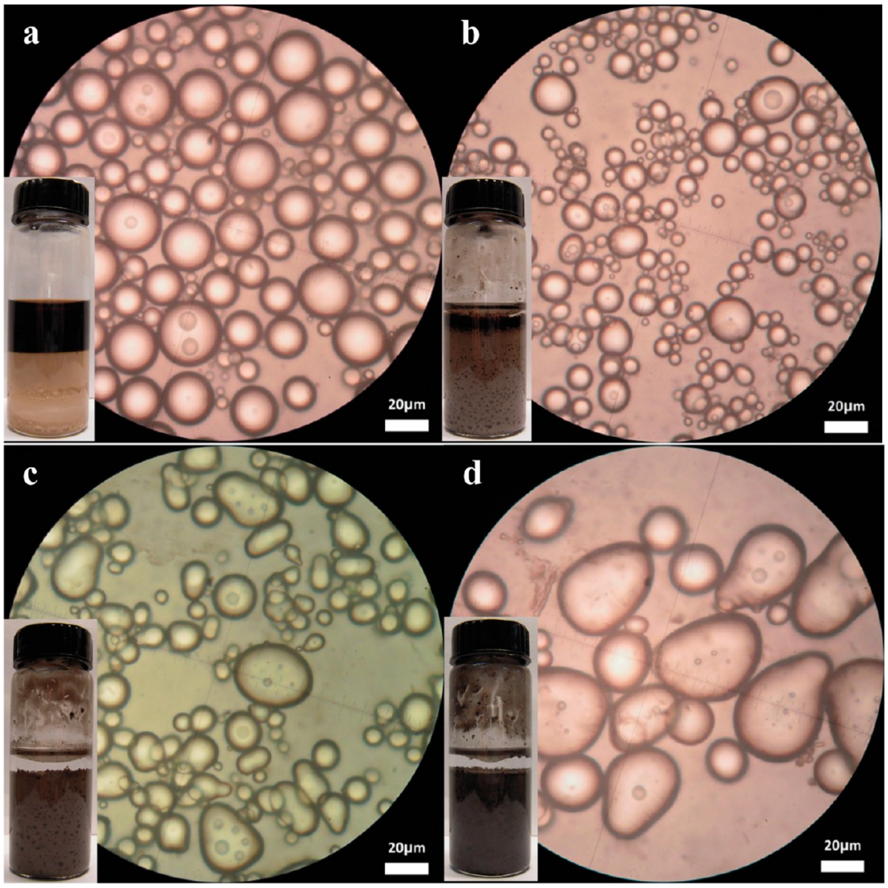

Figure 13. Optical micrographs and photographs 72 h after preparation of Pickering emulsions stabilized by GO slightly reduced to different extents. The maximum absorption peak (λ_{max}) are (nm) (a) 234.8, (b) 241.8, (c) 252.6, and (d) 257.8. GO concentration: 1 mg mL^{-1}. Oil/water ratio: 1:1.

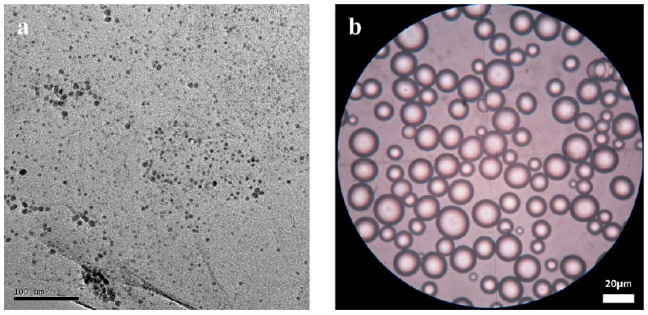

Figure 14. (a) The TEM image of Ag/GO. (b) The optical micrograph of Pickering emulsions stabilized by Ag/GO. Oil/water ratio: 1:2.

product 4-AP. The reduction of 4-NP to 4-AP can be achieved in the presence of $NaBH_4$ without using any catalyst, but it requires about 430 min. When the emulsion stabilized by Ag/GO was added, the reaction was complete in about 7 min.

The reaction kinetics can be easily monitored from the time-dependent absorption spectra. Since the concentration of $NaBH_4$ is very high compared with that of 4-NP, the reaction follows pseudo-first-order reaction kinetics.[47] Thus, the pseudo-first-order rate constant of the reaction can be calculated from the equation $\ln(A_t/A_0) = Kt$, where A_0 and A_t are the absorbance values of 4-NP initially and at time t, respectively, and K is the rate constant. As shown in Figure 15B, the plot of $\ln(A_t/A_0)$ versus time (t) is linear. The rate constant calculated from the slope of the plot is 0.64 min^{-1}. The ratio of rate constant K over the weight of the catalyst was calculated to be 1.43×10^3 s^{-1} g^{-1}, which is much higher than previously reported ratios (1.87 and 11.73 s^{-1} g^{-1}).[48,49]

The recyclability of the catalyst involved in the reduction of 4-NP was also investigated (Figure 16A). The results showed that there was very little loss of catalytic activity for three cycles, but the reaction time increased to 25 min for the sixth cycle, probably as a result of aggregation of the droplets. The optical micrograph of the catalyst after three cycles is shown in Figure 16B. It can be seen that some of the emulsion droplets aggregated together and some of the droplets were broken, which may be responsible for the loss of catalytic activity.

4. CONCLUSIONS

Dispersions of GO sheets were used to prepare stable Pickering emulsions. The type of oil was crucial for the formation of the Pickering emulsion, and aromatic solvents with substituent groups or multiple benzene rings better stabilized the emulsions than other solvents. As the sonication time and GO concentration increased, the average droplet size decreased, but the stable emulsion volume increased. The emulsions tended to achieve good stability at intermediate oil/water ratios and low pH values. In addition, the stability of the emulsions can be dramatically improved by the addition of salt, which causes aggregation of the GO sheets. A divalent electrolyte had a more significant effect than a univalent electrolyte and enhanced the stability of the emulsion at a much lower concentration. A slight reduction of GO also helped increase the stable emulsion volume, but made the shape of the droplets

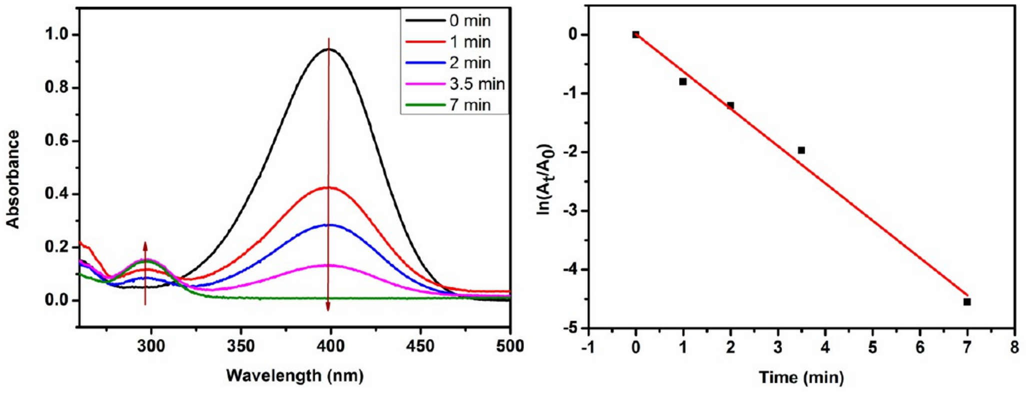

(A) (B)

Figure 15. (A) Time-dependent UV−vis absorption spectra for the reduction of 4-nitrophenol in the presence of emulsion stabilized by Ag/GO as the catalyst. (B) The natural logarithm of the absorbance at 400 nm versus the reduction time.

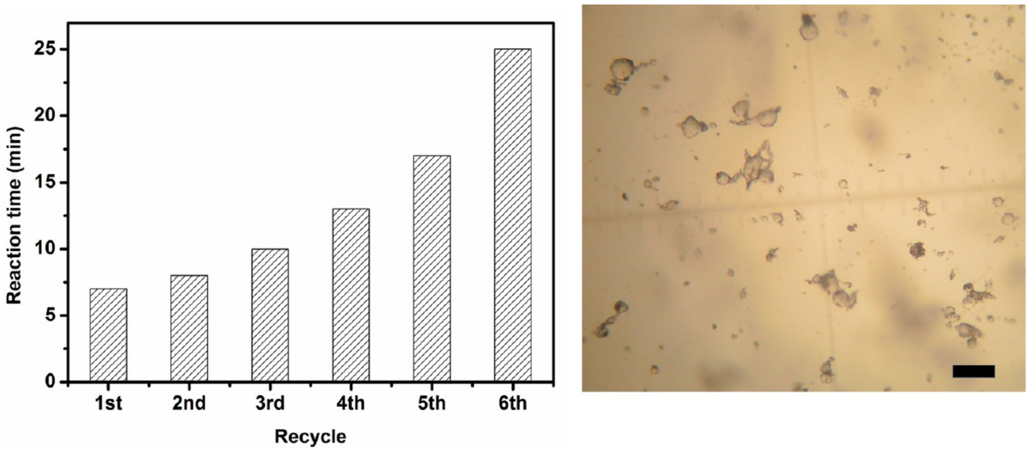

(A) (B)

Figure 16. (A) Recyclability of the emulsions stabilized by Ag/GO for the reduction of 4-nitrophenol. (B) The optical micrograph of the catalyst after three recycles. The scale bar is equal to 100 μm.

irregular. In all solvents, the emulsions were of the oil-in-water type, but interestingly, w/o/w multiple emulsion droplets were also observed under some conditions in the benzyl chloride−water system. A moderate reduction of GO also contributed to the formation of multiple emulsion droplets. The number of multiple emulsion droplets increased with salt concentration, and almost all droplets possessed multiple structures when the NaCl concentration was 500 mM. Multiple emulsion droplets also tended to form at low GO concentrations, low pH values, high oil/water ratios, and high salt concentrations. In addition, a Pickering emulsion stabilized by Ag/GO was also prepared, and it showed good catalytic performance for the reduction of 4-nitrophenol. This research paves the way for the fabrication of graphene-based functional materials with novel nanostructures and microstructures.

■ ASSOCIATED CONTENT

Ⓢ Supporting Information

The TEM images of GO sheets; AFM tap-mode image and height profile of GO; FT-IR spectrum of GO; XRD patterns of graphite and GO; the XPS spectra for GO and the C 1s XPS spectra for GO; optical micrographs of Pickering emulsions stabilized by GO using benzene and benzene with dissolved naphthalene as solvents; optical micrographs and photographs of benzyl chloride-in-water Pickering emulsions stabilized by GO with 7 and 10 min of sonication; photographs of Pickering o/w emulsions stabilized by GO at different concentrations (oil/water ratio: 2:1) of 0.25, 0.5, 1, 3, and 6 mg/mL; and optical micrographs and photographs of Pickering emulsions stabilized by GO with different $MgCl_2$ concentrations (mM) of 0.1, 1, 10, 20, 50, 100, 300, 500, and 1000. This material is available free of charge via the Internet at http://pubs.acs.org.

■ AUTHOR INFORMATION

Corresponding Author

*E-mail: wufei0125@yahoo.cn (F.W.), jianpingg@eyou.com (J.G.).

Notes

The authors declare no competing financial interest.

■ ACKNOWLEDGMENTS

This work was supported by the Tianjin Municipal Science and Technology Commission of the People's Republic of China (09JCZDJC23300), the National Science Foundation of China (Nos. 21074089 and 21276181) and Science and Technology Development Projects for Universities of China (Nos. 20121024).

REFERENCES

(1) Ramsden, W. *Proc. R. Soc. London* **1903**, *72*, 156−164.

(2) Pickering, S. U. *J. Chem. Soc.* **1907**, *91*, 2001−2021.

(3) Dickinson, E. *Curr. Opin. Colloid Interface Sci.* **2010**, *15*, 40−49.

(4) Rayner, M.; Timgren, A.; Sjoo, M.; Dejmek, P. *J. Sci. Food Agric.* **2012**, *92*, 1841−1847.

(5) Frelichowska, J.; Bolzinger, M. A.; Pelletier, J.; Valour, J. P.; Chevalier, Y. *Int. J. Pharm.* **2009**, *371*, 56−63.

(6) Marku, D.; Wahlgren, M.; Rayner, M.; Sjoo, M.; Timgren, A. *Int. J. Pharm.* **2012**, *428*, 1−7.

(7) Chen, H. B.; Zhu, H. D.; Hu, J. D.; Zhao, Y. B.; Wang, Q.; Wan, J. L.; Yang, Y. J.; Xu, H. B.; Yang, X. L. *ACS Nano* **2011**, *5*, 2671−2680.

(8) Melle, S.; Lask, M.; Fuller, G. G. *Langmuir* **2005**, *21*, 2158−2162.

(9) Bon, S. A. F.; Colver, P. J. *Langmuir* **2007**, *23*, 8316−8322.

(10) Yang, H. J.; Cho, W. G.; Park, S. N. *J. Ind. Eng. Chem.* **2009**, *15*, 331−335.

(11) Aveyard, R.; Binks, B. P.; Clint, J. H. *Adv. Colloid Interface Sci.* **2003**, *100*, 503−546.

(12) Binks, B. P. *Curr. Opin. Colloid Interface Sci.* **2002**, *7*, 21−41.

(13) Binks, B. P.; Rodrigues, J. A. *Angew. Chem., Int. Ed.* **2005**, *44*, 441−444.

(14) Madivala, B.; Vandebril, S.; Fransaer, J.; Vermant, J. *Soft Matter* **2009**, *5*, 1717−1727.

(15) Leal-Calderon, F.; Schmitt, V. *Curr. Opin. Colloid Interface Sci.* **2008**, *13*, 217−227.

(16) Binks, B. P.; Lumsdon, S. O. *Langmuir* **2000**, *16*, 8622−8631.

(17) Shen, M.; Resasco, D. E. *Langmuir* **2009**, *25*, 10843−10851.

(18) Binks, B. P.; Fletcher, P. D. I.; Holt, B. L.; Beaussoubre, P.; Wong, K. *Phys. Chem. Chem. Phys.* **2010**, *12*, 11954−11966.

(19) White, K. A.; Schofield, A. B.; Wormald, P.; Tavacoli, J. W.; Binks, B. P.; Clegg, P. S. *J. Colloid Interface Sci.* **2011**, *359*, 126−135.

(20) Nonomura, Y.; Kobayashi, N.; Nakagawa, N. *Langmuir* **2011**, *27*, 4557−4562.

(21) Binks, B. P.; Whitby, C. P. *Colloids Surf., A* **2005**, *253*, 105−115.

(22) Binks, B. P.; Lumsdon, S. O. *Phys. Chem. Chem. Phys.* **1999**, *1*, 3007−3016.

(23) Liu, X. Y.; Yi, C. L.; Zhu, Y.; Yang, Y. Q.; Jiang, J. Q.; Cui, Z. G.; Jiang, M. *J. Colloid Interface Sci.* **2010**, *351*, 315−322.

(24) Yi, C. L.; Yang, Y. Q.; Zhu, Y.; Liu, N.; Liu, X. Y.; Luo, J.; Jiang, M. *Langmuir* **2012**, *28*, 9211−9222.

(25) Wu, C. H.; Chiu, W. Y.; Don, T. M. *Polymer* **2012**, *53*, 1086−1092.

(26) Sturzenegger, P. N.; Gonzenbach, U. T.; Koltzenburg, S.; Gauckler, L. J. *Soft Matter* **2012**, *8*, 7471−7479.

(27) Adelmann, H.; Binks, B. P.; Mezzenga, R. *Langmuir* **2012**, *28*, 1694−1697.

(28) Garcia, P. C.; Whitby, C. P. *Soft Matter* **2012**, *8*, 1609−1615.

(29) de Folter, J. W. J.; van Ruijven, M. W. M.; Velikov, K. P. *Soft Matter* **2012**, *8*, 6807−6815.

(30) van Rijn, P.; Wang, H. H.; Boker, A. *Soft Matter* **2012**, *7*, 5274−5280.

(31) Kalashnikova, I.; Bizot, H.; Cathala, B.; Capron, I. *Langmuir* **2011**, *27*, 7471−7479.

(32) Compton, O. C.; Nguyen, S. T. *Small* **2010**, *6*, 711−723.

(33) Zhu, Y. W.; Murali, S.; Cai, W. W.; Li, X. S.; Suk, J. W.; Potts, J. R.; Ruoff, R. S. *Adv. Mater.* **2010**, *22*, 3906−3924.

(34) Kim, J. Y.; Cote, L. J.; Kim, F.; Yuan, W.; Shull, K. R.; Huang, J. X. *J. Am. Chem. Soc.* **2010**, *132*, 8180−8186.

(35) Gudarzi, M. M.; Sharif, F. *Soft Matter* **2011**, *7*, 3432−3440.

(36) Pardhy, N. P.; Budhlall, B. M. *Langmuir* **2010**, *16*, 13130−13141.

(37) Teixeira, R. F. A.; McKenzie, H. S.; Boyd, A. A.; Bon, S. A. F. *Macromolecules* **2011**, *44*, 7415−7422.

(38) Hummers, W. S.; Offeman, R. E. *J. Am. Chem. Soc.* **1958**, *80*, 1339.

(39) Wu, T.; Wang, X. R.; Qiu, H. X.; Gao, J. P.; Wang, W.; Liu, Y. *J. Mater. Chem.* **2012**, *22*, 4772−4779.

(40) Ashby, N. P.; Binks, B. P. *Phys. Chem. Chem. Phys.* **2000**, *2*, 5640−5646.

(41) Moon, I. K.; Lee, J.; Ruoff, R. S.; Lee, H. *Nat. Commun.* **2010**, *1*, 73.

(42) Wang, S. R.; Zhang, Y.; Abidi, N.; Cabrales, L. *Langmuir* **2009**, *25*, 11078−11081.

(43) Rourke, J. P.; Pandey, P. A.; Moore, J. J.; Bates, M.; Kinloch, I. A.; Young, R. J.; Wilson, N. R. *Angew. Chem., Int. Ed.* **2011**, *50*, 3173−3177.

(44) Zangmeister, C. D.; Ma, X. F.; Zachariah, M. R. *Chem. Mater.* **2012**, *24*, 2554−2557.

(45) Zhang, J. C.; Li, L.; Wang, J.; Sun, H. G.; Xu, J.; Sun, D. J. *Langmuir* **2012**, *28*, 6769−6775.

(46) Guo, Y. Q.; Sun, X. Y.; Liu, Y.; Wang, W.; Qiu, H. X.; Gao, J. P. *Carbon* **2012**, *50*, 2513−2523.

(47) Jana, S.; Ghosh, S. K.; Nath, S.; Pande, S.; Praharaj, S.; Panigrahi, S.; Basu, S.; Endo, T.; Pal, T. *Appl. Catal., A* **2006**, *313*, 41−48.

(48) Ma, H. H.; Geng, Y. Y.; Lee, Y. I.; Hao, J. C.; Liu, H. G. *J. Colloid Interface Sci.* **2013**, *394*, 223−230.

(49) Wang, C. H.; Tang, K. B.; Wang, D. K.; Liu, Z. P.; Wang, L. L. *J. Mater. Chem.* **2012**, *22*, 22929−22934.